Experimental Tests and Numerical Modelling on Slender Steel Columns at High Temperatures

Jean-Marc Franssen[a], Bin Zhao[b] and Thomas Gernay[c]

[a] Structural Engineering Department, University of Liege, Quartier Polytech 1, allee de la Decouverte 9, 4000 Liege, Belgium, jm.franssen@ulg.ac.be

[b] C.T.I.C.M., Espace technologique, L'orme des merisiers, Immeuble Apollo, 91193 Saint-Aubin, France, France

[c] The National Fund for Scientific Research F.R.S.-FNRS, Structural Engineering Department, University of Liege, Quartier Polytech 1, allee de la Decouverte 9, 4000 Liege, Belgium, thomas.gernay@ulg.ac.be

ABSTRACT

Purpose: The objective of this research work is to gain from experimental tests an insight into the failure mode of slender steel columns subjected to fire. The tests will also be used to validate a numerical model.

Methodology: A series of experimental fire tests were conducted on eight full scale steel columns made of slender I shaped class 4 sections. Six columns were made of welded sections (some prismatic and some tapered members) and two columns were made of hot rolled sections. The nominal length of the columns was 2.7 meters with the whole length being heated. The load was applied at ambient temperature after which the temperature was increased under constant load. The load was applied concentrically on some tests and with an eccentricity in other tests. Heating was applied by electrical resistances enclosed in ceramic pads. Numerical simulations were performed with the software SAFIR® using shell elements.

Findings: The tests have allowed determining the appropriate method of application of the electrical heating system for obtaining a uniform temperature distribution in the members. Failure of the columns during the tests occurred by combination of local and global buckling. The numerical model reproduced correctly the failure modes as well as the critical temperatures.

Value/Originality: The numerical model that has been validated has been used in subsequent parametric analyses performed in order to derive design equations to be used in practice. This series of test results can be used by the scientific community to validate their own numerical or analytical models for the fire resistance of slender steel columns.

Keywords: Steel; Column; Class 4; Slender section; Fire resistance; Test; Modelling.

1. INTRODUCTION

When stocky steel members are submitted to compression or bending, they deform globally, which means that their longitudinal axis is shortened or bent but their section does not change in shape. Members made of slender plates, on the contrary, distort on the whole length and may also exhibit short waves distortions. Such behaviour is much more complex than the behaviour of stocky sections and this is the reason why design methods for slender members are lagging behind design methods developed for other members. Eurocode 3 [1], for example, recommends that the temperature in Class 4 sections should be designed according to a method that is a direct extrapolation of a method developed for room temperature, the extrapolation being based on reasonable but unverified hypotheses. Alternatively, the steel temperature should not exceed 350°C.

In order to fill the lack of knowledge about slender elements behaviour at elevated temperatures, a European research project called FIDESC4 has been funded by the RFCS. This project involves experimental testing, parametric numerical analyses and development of simple design rules. The present paper reports the characteristics and the results of the FIDESC4 experimental test campaign performed at the University of Liege on slender steel columns at elevated temperatures.

2. TEST SET-UP

2.1 Heating of the specimens

The specimens were heated on the whole length but not in a gas furnace used for standard fire resistance tests. It was preferred to heat the specimens with electric resistance inserted in ceramic pads, see Figure 1, for the reasons detailed below.

In order to allow for a better comparison of the structural behaviour between all specimens, it was desired to follow the same temperature increase rate in all specimens, independent of the thermal massivity of the specimen. If the standard fire curve is applied in the furnace, different specimens with different massivity will heat up at different rates. On the other hand, it is difficult to control the rate of temperature increase in the steel specimen with a gas furnace. Such furnaces are normally designed to follow the standard fire curve, which means that a significant amount of power is released in the furnace as soon as the burners are turned on in order to cope with the rapid temperature increase shown by the standard ISO834 fire curve during the first instants of the test. The electric heating system is designed to follow a prescribed temperature heating rate directly measured on the steel specimen.

Another reason for using electric heating is that this allows a more uniform temperature distribution in the specimens. A gas furnace is indeed heated by a discrete number of burners, the location of which can induce a non-uniform temperature distribution in the specimen because of the radiation of the flame of each burner. In addition to that, the gas burners may

not be evenly distributed around the specimen. The ceramic pads, on the contrary, are easily distributed symmetrically around the specimens.

A series of blank tests was nevertheless performed on an unloaded specimen. The first reason was to verify that the thermal insulating blankets that had been installed surrounding the specimen and the ceramic pads would be sufficient to generate the desired heating rate until the desired maximum temperature. It is noted that the ceramic pads are installed inside the blankets (close to the specimen); hence the purpose of the insulating blankets here is to allow for a proper heating of the specimen and not to model any kind of fire insulation. The second reason was to verify the uniform character of the temperature distribution in the steel specimen. In the first tests, a significant temperature difference was observed in the web of the section between the zones that were directly covered by a ceramic heating pad and the zone that were not covered (it is not possible to cover all the surface of the specimen with ceramic pads; some zones are covered while some zones are not covered). With a heating rate of 100°C/hour, temperature differences in the order of 50 to 80 degrees Celsius were observed for two locations in the web separated by only 130 mm. Decreasing the heating rate or allowing for some minutes of constant temperature at, say, every 100°C step, did not prove to solve the problem. The problem was solved when a practical arrangement was found that allowed the ceramic pads not to be in direct contact with the steel specimen. A gap of around 10 mm was provided between the pads and the steel section and it appeared as if convection in this gap surrounding the column reduced very significantly the temperature differences. With a heating rate of 100°C/h up to 300°C and 200°C/h up to 600°C, the maximum temperature difference was, at the end of the test, only 27°C. The tests of the loaded specimen were thus performed at a heating rate of 200°C/h, with the heating pads separated in 6 different zones, each zone being controlled independently.

Figure 1. The heating system consists of electric resistances inserted in ceramic pads

Finally, it is much easier to measure lateral displacements of the column with the electric system than in a gas furnace. Two rods were inserted through the insulating blankets at mid-level of the column, in perpendicular directions. The horizontal displacements in two directions could thus be measured and even the global buckling mode could be visually observed in the last instants before failure, which helped in the decision process leading to the unloading of the specimen before excessive damage is induced in the equipment.

2.2 Loading of the specimens

Each specimen was fabricated with a stiff steel end plate welded at each end of the column; the thickness of the plate varied from 20 to 35 mm. In these plates were drilled 4 holes which allowed bolted connection with another steel plate that was part of a hinge support. The distance between the axis of the hinge and the end plate of the hinge was 132.5 mm. Between the two steel plates were inserted two plates of high density insulating material (15 + 20 mm, Promatect-H) in order to limit the heat losses from the specimen to the support, see the clearer plates on Figure 2. Such heat loss would indeed generate a non-uniform temperature distribution along the column length and, potentially, damage the hinge. The insulating product has an average compressive strength in the order of 4 N/mm² up to 600°C.

The hinges were assumed to provide no restrain to rotation around one axis while preventing the rotation around the perpendicular axis. Preliminary numerical simulations performed with shell finite elements of the code SAFIR [2] showed that such support conditions were sufficient to induce failure in the direction of the strong axis of the section; no torsional compression buckling or buckling in the direction of the weak axis would occur (except when this is desired and the section is turned by 90 degrees). It was thus not necessary to provide mechanical means of lateral restraint that would have divided in two the buckling length in the direction of the weak axis.

Figure 2. Hinged support

2.3 Test procedure

The specimen was first loaded at room temperature and the load was thereafter kept constant for 15 minutes. The temperature in the steel column was then increased at a constant rate while the load was maintained (longitudinal thermal expansion was not restrained).

Applied load, temperature in the steel member at different point, as well as axial displacement and two transverse displacements at mid-level were recorded continuously.

The temperature was increased until the hydraulic system could not maintain the load constant in the hydraulic jack. At this time, axial and lateral displacements exhibit a rapid increase and the development of global buckling was clearly visible.

The test set-up is shown in Figure 3. The column, wrapped in ceramic mats, is installed in the testing frame; displacement transducers are used for measuring lateral displacements.

Figure 3. Test set-up

3. TESTED MEMBERS

Eight columns were tested, some with the load applied eccentrically, at one end or at both ends, and some with nominally axial loading. In fact, a small eccentricity of 5 mm was systematically applied in order to induce buckling in the direction of the weak axis and, also, in order to decrease the relative value of the uncertainty that nevertheless exists on the positioning of the load. This uncertainty is estimated to be in the order of 1 mm. The eccentricity was applied by shifting laterally the hinge fixed to the end plates of the columns, see Figure 4, with respect to the axis of the column. The two hinges were located in the plane of symmetry of the loading frame, see Figure 3. The test arrangements were as described in Table 1. The values given for the section correspond respectively to the section height, flange width, web thickness and flange thickness, in mm.

Table 1. Test arrangements.

Test no.	Section	Class of the web	Class of the flange	Eccentricity[*] [mm] and direction	Applied load [kN]
1	IPE240AA 237/120/5.2/8.3	4	1	5 – 5, weak	144.5
2	450/150/4/5	4	4	5 – 5, weak	122.4
3	450/150/4/5	4	4	5 – 5, weak	204.0
4	500-300/300/4.5/5	4	4	6 – 6, strong	348.0
5	360/150/4/5	4	4	71 – 71, strong	231.3
6	360/150/4/5	4	4	177.5 – 177.5, strong	166.4
7	HE340AA 320/300/8.5/11.5	3	3	100 – 0, strong	760.8
8	450-300/150/4/5	4	4	150 – 0, strong	219.0

[*] Measured values after installation of the column in the test rig.

Two tests were performed on hot rolled sections, four tests on prismatic welded sections and two tests on tapered welded sections. The nominal length of all specimens was 2700 mm measured from end plate to end plate (that is, not counting the thickness of the plates). The hinge supports were always turned in such a way to favour buckling in the direction of the applied eccentricity (rotation allowing displacements in the direction of the eccentricity and preventing displacements in the other direction).

Initial geometrical imperfections were measured for each specimen in the web and in each flange. The imperfection measurements were performed manually using a ruler (a straight aluminium bar taken as a reference). The ruler was placed along the web and along both flanges of the columns. Then, the clearance between the ruler and the specimen was measured

every 10 centimetres in the direction of the length. The two extremities of the columns were taken as a reference in the derivation of the imperfection (meaning that the imperfection was assumed to be null at the extremities, and the measurements were corrected accordingly). This process yielded a profile for the imperfections along the length of the columns. From this profile, amplitudes of the global and local imperfections can be deduced assuming a sinusoidal distribution for the global imperfection. Table 2 gives the amplitude of the global imperfections in mm measured in the direction of the weak axis and of the local imperfections in the web and in the flange.

Table 2. Geometrical imperfections and material properties.

Test no.	Length [mm]	Geometrical imperfection [mm]			Yield strength [N/mm²]	
		Global	Local in web	Local in flange	Web	Flange
1	2 740	1.5	0.2	0.3	445.5	397.8
2	2 760	2.7	3.2	2.4	464.7	404.0
3	2 760	5.4	2.7	4.7	464.7	404.0
4	2 750	1.8	4.5	1.5	-	-
5	2 760	2.2	3.4	1.6	-	-
6	2 760	1.0	2.2	1.2	464.7	404.0
7	2 755	1.5	0.5	0.6	579.5	530.5
8	2 760	1.0	2.8	1.5	464.7	404.0

Table 2 also gives the measured yield strength for the web and for the flange and the length of the column (including the end plates). Note that the webs of columns no. 2, 3, 6 and 8 have been produced from a same 4 mm thick steel plate, and the flanges of these columns have been produced from a same 5 mm thick plate, which explains why identical values of yield strength are indicated in Table 2 for these columns. No coupon tests were available for tests 4 and 5; for the numerical simulation it was assumed that the steel yield strength for these columns is the same as for column no. 3.

4. TEST RESULTS

Table 3 gives the temperature reached at time of failure and the main features of the failure mode. The deformed shape of columns 4 and 7 after failure are shown in Figure 4 and 5, respectively. As can be seen, these slender columns have exhibited local instabilities (distortions) under high temperatures.

Failure was deemed to occur when axial and lateral displacements exhibited a rapid increase and the load in the hydraulic jack could not be maintained constant anymore by the hydraulic system. At this time, the development of global buckling was clearly visible.

In the philosophy of *open data*, more data such as temperature-displacement curves or pictures of the columns after failure can be found on http://hdl.handle.net/2268/163773.

In the tests, the location along the length of the column of the zones that exhibit local buckling has been influenced by the global buckling of the column (which tends to locate these zones at mid-level of the column) but also by the local amplitude of initial imperfections which may trigger local buckling slightly away from mid-level.

Table 3. Critical temperatures and failure mode.

Test no.	Temperature [°C]		Failure mode in the tests
	from the tests	by SAFIR	
1	610	572	Global in the weak axis direction, no local buckling
2	608	594	Global in the weak axis direction, local buckling in the flanges
3	452	459	Global in the weak axis direction, local buckling in the flanges
4	520	535	Global in the strong axis direction, local buckling in the flanges, lateral torsional buckling at mid-level
5	510	526	Global in the strong axis direction, local buckling in the flanges
6	530	531	Essentially local buckling
7	623	630	Global in the strong axis direction, local buckling in the flanges and in the web approximately at mid-level
8	505	537	Local buckling in the flange, some lateral torsional buckling at mid-level

Figure 4. Tested column no. 4 after failure.

Figure 5. Tested column no. 7 after failure.

5. NUMERICAL SIMULATIONS

The tests were modelled first before the tests, based on the nominal characteristics of the material properties. These simulations served first to indicate the type of failure mode to be expected and they showed that it was not necessary to provide lateral restrain at mid-level of the column to force the global buckling in the desired direction: the applied eccentricity and the difference in restrain with respect to rotation in both axes provided by the hinges would be sufficient to induce failure in the desired direction. The simulations also served to choose the load to be applied during the test in order to obtain failure in the desired temperature range (from 500 to 600 degrees Celsius).

After the tests, simulations were performed again based on the measured values of the yield strength, of the steel temperature, of the applied load and of the applied eccentricity. The geometrical imperfections were simplified and represented by half a sinusoidal in the direction of the weak axis for the global imperfection and sinusoidal waves for the flanges and for the web. Figure 6 illustrates the initial geometry of a specimen, with the imperfections being amplified to be more visible. The columns were modelled in shell finite elements using 8 elements on the flange width, 8 elements on the web height and 100 elements on the length.

In order to get the correct buckling length of the column, the nominal length presented in Table 2 was increased by 167.5 mm at each end of the column in order to take into account the extra length provided by the insulating plates (35 mm) and by the hinge (132.5 mm). These extra lengths were modelled by rigid extensions in order to take into account the fact that no local buckling can develop in these regions.
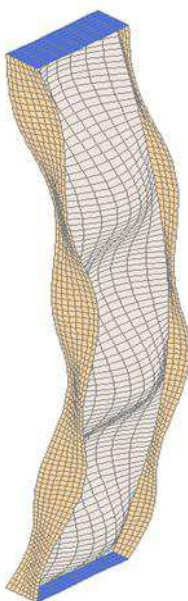

Figure 6. Geometrical imperfections

The critical temperatures obtained by numerical simulation are presented in Table 3. The simulations were able to capture the failure mode exhibited by the columns. In particular, local instabilities in the flanges and in the web can be captured by the model, see for instance the deformed shape at failure for column no. 4 on Figure 7 (failure mode to be compared with Figure 4). Figure 8 presents the comparison between experimental results and numerical results in terms of critical temperature. The average value of the ratio SAFIR/Test is 1.01 with a standard deviation of 0.04. The numerical model validated by this comparison is presently being used in a series of parametric analyses performed in order to generate a data base of results. This data base will be used to develop and validate a design method for the fire resistance of slender columns.
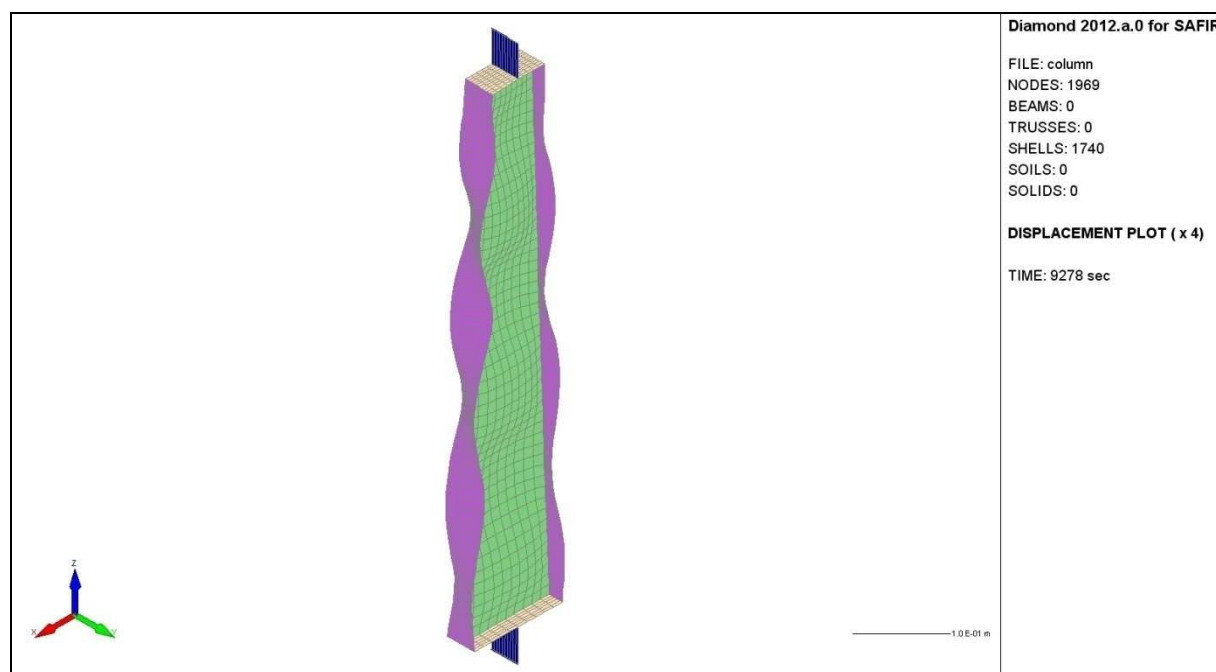

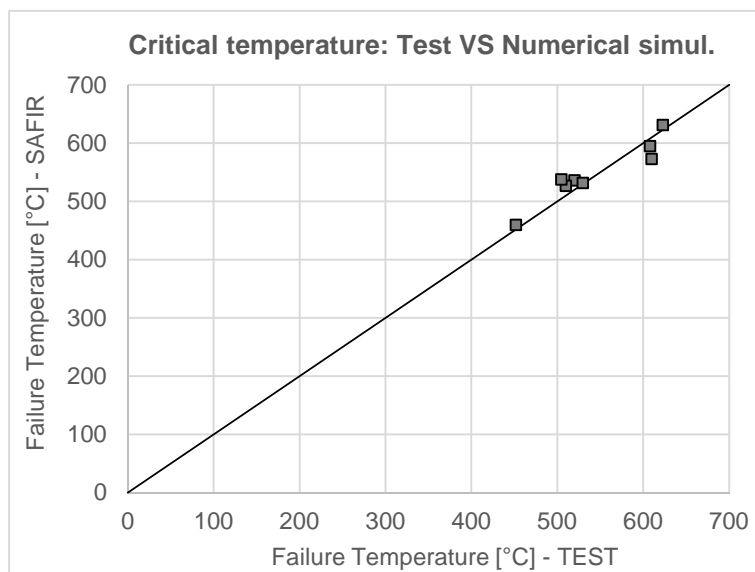Figure 7. Deformed shape at failure obtained by numerical simulation for column no. 4

Figure 8. Comparison between experimental tests and numerical simulations

6. CONCLUSION

A series of eight full scale experimental tests has been performed on slender steel columns under increasing temperature. This experimental campaign aims at improving the understanding of slender elements behaviour at elevated temperatures. The test set-up, tested specimens, testing procedure and test results are documented, for the essential features in this paper and for all details in an *open data* philosophy.

The heating system consisting of electric resistances inserted in ceramic pads proved efficient for heating the specimens uniformly at a predefined temperature increase rate provided that the ceramic pads are not in direct contact with the steel specimen. The tested steel columns, made of European class 4 sections, exhibited local distortions under high temperatures. Eventually, global buckling was observed at the time of failure.

Numerical simulations by nonlinear finite element analysis were conducted with the software SAFIR®. Shell elements were selected for their ability to model the local instabilities in the sections. The simulations were able to capture the behaviour of the steel columns, in particular the failure mode and the temperature at failure.

These tests increase our knowledge about the failure modes of slender columns. They may also serve as a validation base of numerical models and design models.

ACKNOWLEDGEMENT

REFERENCES

[1] European Committee for Standardization**,** Eurocode 3 - Design of steel structures - Part 1-2: General rules – Structural fire design, Brussels, 2005.

[2] Franssen, J.-M., SAFIR: A Thermal/Structural Program for Modeling Structures under Fire, Engineering Journal, American Institute of Steel Construction Inc, 2005, 42(3), 143-158. http://hdl.handle.net/2268/2928